The Be-Cu (Beryllium-Copper) System

9.01218 63.546

By D.J. Chakrabarti
Alcoa Laboratories
D.E. Laughlin
Carnegie Mellon University
and
L.E. Tanner
Lawrence Livermore Laboratory

Equilibrium Diagram

The assessed Cu-Be phase diagram with select experimental data is shown in Fig. 1. The equilibrium phases at 1 atm are:

- The liquid, (L), which is miscible at all compositions.
- The fcc (Cu) terminal solid solution, which is stable up to the melting point of Cu at 1084.87 °C [Melt], with a maximum solubility of 16.5 at.% (2.73 wt.%) Be at 866 °C.
- The bcc disordered solid solution, β, which is stable above ~620 °C; this phase is formed by a peritectic transformation at 866 °C on the Cu-rich side and probably also at 930 °C on the Be-rich side. It may also form congruently from the liquid at 860 °C.
- The simple cubic, γ ($B2$, CsCl type), ordered phase (also designated β' in the literature), which is stable over a narrow phase field at off-equiatomic, Be-deficient compositions. This phase is formed presumably by a higher order transition from β above the critical point at 880 °C and below that by spinodal transformation, inside the two-phase field. It is formed eutectoidally at ~620 °C and below that by precipitation from (Cu) via several intermediate metastable phases.
- The Laves-type fcc phase, δ, with a broad phase field that extends from ~64.3 at.% Be at 930 °C to ~81.5 at.% Be at 1109 °C and up to 1219 °C, where it is formed by congruent transformation.
- The bcc (βBe) allotropic modification, which is stabilized by the presence of Cu from its melting point at 1289 °C down to 1109 °C at ~13.7 at.% Cu; the maximum solubility of Cu in (βBe) is 17.3 at.% at 1199 °C.
- The cph (αBe) terminal solid solution, which extends up to 9.5 at.% Cu at 1109 °C and transforms congruently to (βBe) at ~1275 °C.

The various transformations and corresponding equilibrium temperatures and compositions are presented in Tables 1 and 2.

Fig. 1 Assessed Cu-Be Phase Diagram with Select Experimental Data

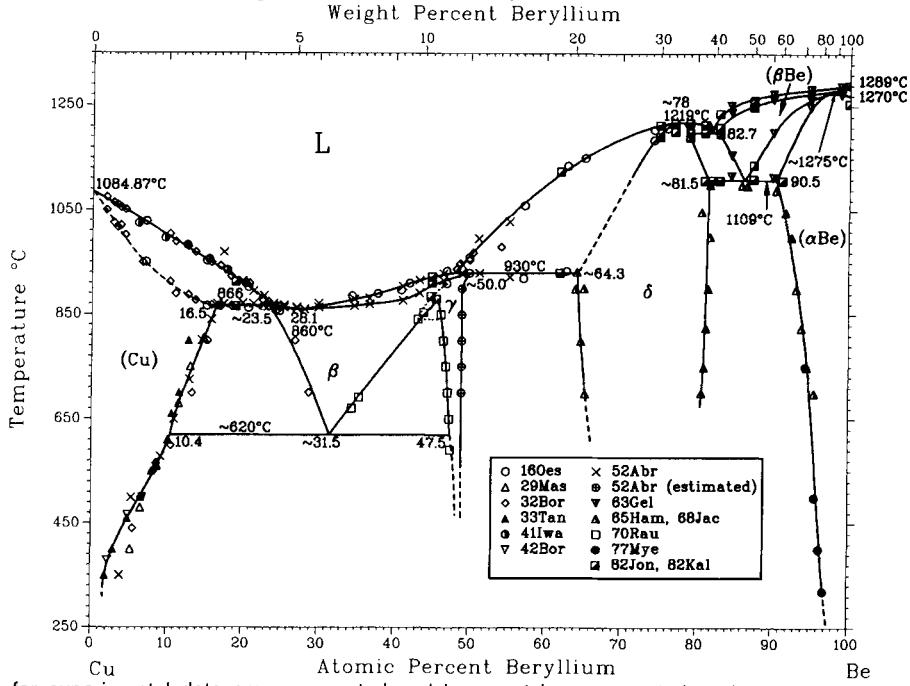

Temperatures shown for experimental data are as reported and have not been corrected to the 1968 temperature scale (IPTS-68). (Experimental methods—thermal analysis [16Oes, 32Bor, 41Iwa, 52Abr, 63Gel, 82Jon, 82Kal]; microscopy [32Bor, 52Abr]; X-ray [33Tan]; electrical resistivity [29Mas, 32Bor]; dilatometry [42Bor]; diffusion couple and EPMA [65Ham, 68Jac].)

D.J. Chakrabarti, D.E. Laughlin and L.E. Tanner, 1987.

Table 1 Special Points of the Assessed Cu-Be Phase Diagram

Reaction	Compositions of the respective phases, at.% Be			Temperature, °C	Reaction type	Reference (a) Composition	Reference (a) Temperature
L + (Cu) ⇄ β	~24	16.5	~23.5	866	Peritectic	[52Abr]; [32Bor]; (b)	[16Oes, 32Bor, 41Iwa, 79Ald]
β ⇄ (Cu) + γ	~31.5	10.4	47.5	620	Eutectoid	[79Ald] (b)	[79Rio]
L ⇄ β		28.1		860	Congruent point	[52Abr]	[52Abr]
γ ⇄ γ_1 + γ_2		45.8		880	Critical point	[70Rau]	[70Rau]
L + δ ⇄ β(?)/L + δ ⇄ γ(?)	48.0	64.3	~50	930	Peritectic	[32Bor, 52Abr]; [52Abr]; [65Ham, 79Ald, 82Jon]	[16Oes, 42Los, 52Abr, 79Ald]
(βBe) ⇄ δ + (αBe)	~86.3	~81.5	90.5	1109	Eutectoid	[65Ham]; [82Jon]; [65Ham]	[82Jon]
L ⇄ δ		~78		1219	Congruent point	[79Ald]	[82Jon]
L ⇄ δ + (βBe)	~82	78.8	82.7	1199	Eutectic	[82Jon]	[82Jon]
(βBe) ⇄ (αBe)		97.8		1275	Congruent point	[63Gel] (c)	[63Gel]

(a) Composition references, when shown separated by semicolons, refer to respective phase compositions given in column 2 in the same order of their occurrence. (b) Extrapolated value. (c) Interpolated value.

Table 2 Additional Experimental Results for Cu-Be Reactions

Reaction	Compositions of the respective phases, at.% Be			Temperature, °C	Reaction type	Reference (a) Composition	Reference (a) Temperature
L + (Cu) ⇄ β	24.1	16.4	23.6	865	Peritectic	[79Ald]	[65Ham]
	···	16.6	···	870	Peritectic	[52Abr]	[52Abr]
				862	Peritectic		[42Los]
β ⇄ (Cu) + γ	31	10	47.4	614 to 624	Eutectoid	[32Bor, 29Mas, 16Oes]	[82Gar]
				~605	Eutectoid		[79Ald]
	31	9.1	48		Eutectoid	[52Abr]	
	31.8	9.7	47.6	580	Eutectoid	[41Iwa]	[74Auv]
				590	Eutectoid		[70Rau]
				605 to 610	Eutectoid		[65Mor]
				608	Eutectoid		[50Fil]
				601 to 618	Eutectoid		[44Tho]
				573	Eutectoid		[41Iwa]
				576	Eutectoid		[32Bor]
				578	Eutectoid		[16Oes, 42Los]
γ ⇄ γ_1 + γ_2		···		885	Critical point		[79Ald]
		···		890	Critical point		[52Abr]
L + δ ⇄ β(?)	47.8	50.8	···	933	Peritectic	[70Ald]; [65Ham, 82Jon]; ···	[65Ham, 32Bor]
L + δ ⇄ γ(?)	48.4	49.6	···	933	Peritectic	[82Jon]; [32Bor]; ···	[65Ham, 32Bor]
(βBe) ⇄ δ + (αBe)	82.7	···	92.5	1117	Eutectoid	[50Kau]	[63Gel]
				1148	Eutectoid		[42Los]
L ⇄ δ		···		1239	Congruent point		[79Ald, 16Oes]
				1215	Congruent point		[32Bor]

(a) Composition references, when shown separated by semicolons, refer to respective compositions given in column 2 in the same order of their occurrence.

Liquidus and Solidus. For the most part, the liquidus has been fairly well established through thermal analysis measurements. The solidus is less well defined, because these measurements, except for those of [63Gel], [82Jon], and [82Kal], were obtained during cooling. Detailed reviews of the early works are given in [Hansen], [49Ray], and [79Ald].

For the liquidus between 0 and ~25 at.% Be, the data of [16Oes], [32Bor], [41Iwa], and [52Abr] are in good agreement, and the accepted liquidus is drawn through them, as shown in Fig. 2 and Table 3. Between ~25 and 48 at.% Be, the liquidus is based on the data of [52Abr] and a single thermal point from [82Kal]. Results of [16Oes], [32Bor], and [41Iwa] in this region indicate unrealistic phase relationships. The existence of a minimum in the β liquidus and solidus (congruent point) was suggested by [16Oes], [32Bor], and [42Los]. The accepted value of 28.1 at.% Be and 860 °C is based on [52Abr]. The data of [16Oes], [32Bor], [52Abr], and [82Kal] are in fair agreement between 45 and 65 at.% Be, and the accepted liquidus is drawn through them (see Fig. 1). Almost no data are available between 65 and ~75 at.% Be for either the liquidus or the solidus.

The high-temperature section of the phase diagram between 75 and 85 at.% Be is based primarily on the works of [82Jon] and [82Kal]. Alloys were made from 99.65 wt.% Be and electrolytic Cu. DTA, X-ray, microscopy, and microprobe analysis techniques were used. The δ phase was indicated to melt congruently at 1219 °C at about 78 at.% Be (see Fig. 3). This is consistent with the thermal arrest data of [16Oes] near this composition and the liquidus maximum observed by [32Bor] at 1215 °C near the $CuBe_3$

Fig. 2 Cu-Be Liquidus and Solidus at the Cu-Rich End of the Cu-Be Phase Diagram

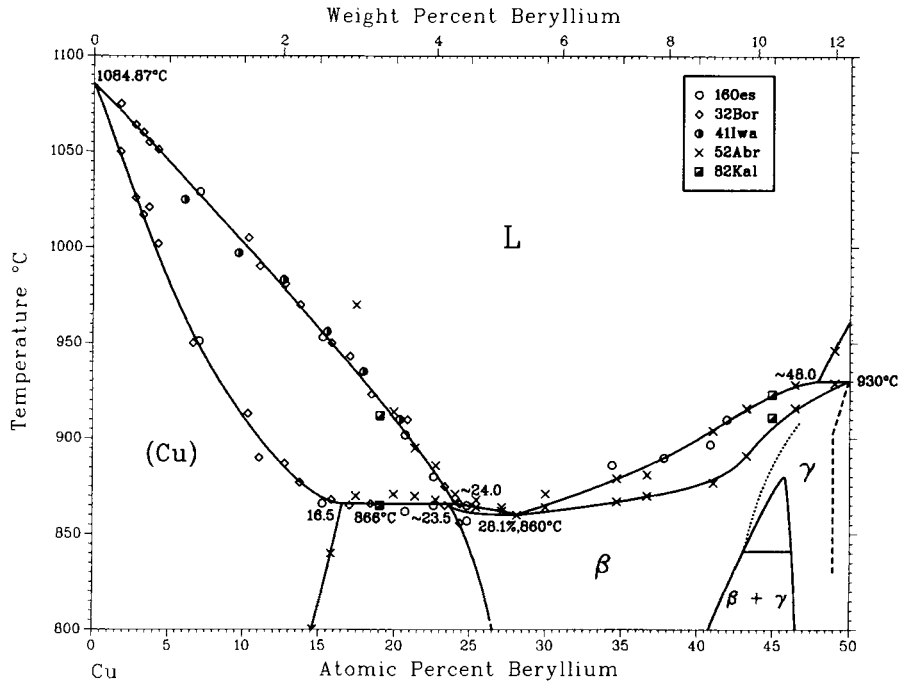

D.J., Chakrabarti, D.E. Laughlin and L.E. Tanner, 1987.

Table 3 Cu-Be Liquidus and Solidus Data

Reference	Composition, at.% Be	Liquidus temperature, °C	Solidus temperature, °C
[16Oes]	7.03	**1029**	**951**
	15.2	**953**	**866**
	20.66	**902**	862
	22.55	880	865
	24.8	865	857
	34.4	886	···
	37.8	**890**	···
	40.9	897	···
	42	**910**	···
[32Bor]	1.7	**1075**	**1050**
	2.7	**1064**	**1026**
	3.2	**1060**	**1017**
	3.6	**1055**	1021
	4.2	**1051**	**1002**
	6.6	···	950
	10.25	**1005**	**913**
	11.0	**990**	890
	12.7	**981**	**887**
	13.7	**970**	**877**
	15.8	**950**	**868**
	17.0	**943**	865
	18.4	**923**	**866**
	20.8	910	**866**
	23.3	**875**	865
	24.3	**866**	856
[41Iwa]	6.0	1025	···
	9.6	997	···
	12.6	**983**	···
[41Iwa](cont'd)	15.5	**956**	···
	17.9	935	···
	20.3	**910**	···
[52Abr]	17.4	970	870
	19.9	**914**	871
	21.3	**895**	870
	22.7	886	868
	24.0	871	867
	25.4	868	864
	27.1	**864**	**862**
	28.1	**860**	**860**
	30.0	**871**	**864**
	34.7	**879**	**867**
	36.7	**881**	**870**
	41.1	**904**	**877**
	43.3	**916**	**891**
	46.5	**928**	**916**
	49.1	**946**	929
[82Kal]	19	917 to 907	867 to 863
	45	926 to 920	911 (h)
	62	1125 to 1123	931 to **930**
[82Jon, 82Kal]	75	1216 to 1211	1191 (h)
	77	1219 to 1215	1201 (h)
	79	1220 to 1216	**1199** (h, c)
	81	1214 (h, c)	**1199** (h, c)
	83	1237 to 1235	1209 (h)
		1262 to 1258	1247 (h)

Note: Accepted results are shown in boldface. The upper and lower temperature limits in the data of [82Kal] and [82Jon] represent results obtained from heating (h) and cooling (c) curves in DTA, respectively. Data from other references are also based on thermal analysis, but from cooling curves only.

Fig. 3 Section of Cu-Be Phase Diagram at the Be-Rich End of the Cu-Be Phase Diagram

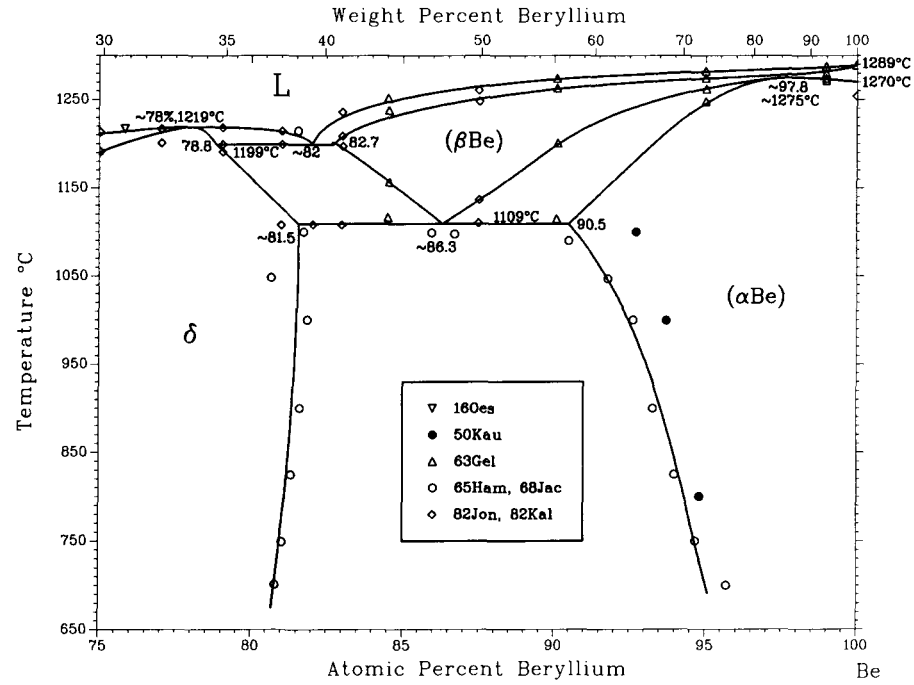

D.J. Chakrabarti, D.E. Laughlin and L.E. Tanner, 1987.

Fig. 4 Solvus of the Primary Solid Solution, (Cu), in the Cu-Be System

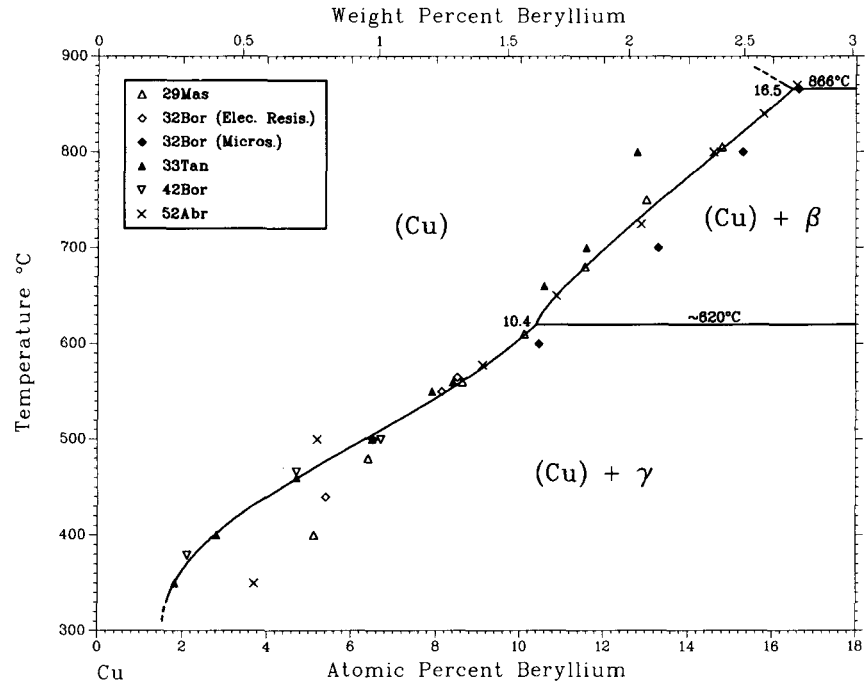

D.J. Chakrabarti, D.E. Laughlin and L.E. Tanner, 1987.

Table 4 Solid Solubility of Be in (Cu)

Reference	Method	Temperature, °C	Composition, at.% Be	Composition, wt.% Be
[29Mas]	Electrical conductivity	800 to 810	**14.8**	2.4
		750	13.03	2.08
		680	**11.56**	1.82
		610	**10.11**	1.57
		560	**8.62**	1.32
		480	6.40	0.96
		400	5.12	0.76
[32Bor]	Microscopy	866	16.65	2.75
	Interpolated value	800	15.3	2.5
		700	13.30	2.13
		600	10.46	1.63
	Electrical resistivity	565	**8.5**	1.3
		550	**8.13**	1.24
	Microscopy	500	6.52	0.98
	Electrical resistivity	440	5.4	0.8
[33Tan]	Lattice parameter	800	12.80	2.04
		700	11.6	1.8
		660	10.6	1.7
		560	8.4	1.3
		550	**7.9**	**1.2**
		500	**6.5**	**1.0**
		460	**4.7**	**0.7**
		400	**2.8**	**0.4**
		350	**1.8**	**0.26**
[42Bor]	Dilatometry	500	**6.7**	1.0
		466	**4.7**	0.7
		379	**2.1**	0.3
[42Los]	Dilatometry, thermal, and microscopy	R.T.	4.7	0.7
		846	16.4	2.7
[52Abr]	Microscopy	870	16.6	2.75
		840	**15.8**	2.59
		800	**14.6**	2.37
		725	**12.9**	2.06
		650	**10.9**	1.71
		578	**9.1**	1.40
		500	5.20	0.77
		350	<3.75	<0.55

Note: Accepted results are shown in boldface.

Table 5 Solid Solubility of Cu in (αBe)

Reference	Method	Temperature, °C	Composition, at.% Cu
[65Ham, 68Jac]	EPMA (a)	1090	9.5
		1048	8.2
		1000	7.35
		900	6.7
		825	6.0
		750	5.3
		700	4.3
[77Mye] (b)	Ion backscattering analysis	750	5.5 ± 1.0
		500	4.25
		400	3.62
	Neon irradiated	320	3.0

(a) EPMA = Electron Probe Micro-Analysis. (b) ±15% accuracy.

composition. A higher liquidus temperature (1239 °C) at $CuBe_3$ composition was indicated by [42Los], but their liquidus data have been known to be systematically higher at other compositions. [82Jon] obtained a three-phase eutectic equilibrium between the L, δ, and (βBe) phases at 1199 °C, compared to 1150 °C reported earlier by [42Los]. The temperature for the eutectoid reaction (βBe) $\rightleftarrows$ δ + (αBe) obtained by them was 1109 °C, as compared to 1117 °C by [63Gel] and 1090 ± 5 °C by [65Ham]. The eutectoid temperature given by [82Jon] is accepted in this evaluation, being intermediate to the results of [63Gel] (based on DTA measurements during heating but using less pure materials) and of [65Ham] (using higher purity materials, but based on a less definitive method, i.e., the diffusion couples).

Both the liquidus and the solidus above ~85 at.% Be and the corresponding solvus were determined by [63Gel] using relatively high-purity Be (combined metallic and interstitial impurities of ~0.06 wt.%) and thermal analysis measurements during heating (Fig. 3).

The (Cu) solidus is based on the data of [32Bor], which is also consistent with the limited data of [16Oes] (see Fig. 2 and Table 3). The accepted peritectic compositions and the temperature invariant at 866 °C are derived from the thermal arrest results of [16Oes], [52Abr], and [82Kal]. Between ~25 and 48 at.% Be, the solidus of the β phase is based on the only available data of [52Abr] (see Fig. 1 and 2). The peritectic invariant at 930 °C is accepted from the thermal arrest results of [16Oes], [52Abr], and [82Kal]. The δ solidus between 65 and 75 at.% Be is tentative and is based on the limited data of [16Oes], [32Bor], and [82Jon]. The (βBe) solidus is based on the works of [63Gel] and [82Jon] as discussed earlier.

The melting points of Cu and Be are 1084.87 and 1289 °C, respectively [Melt]. The βBe $\rightleftarrows$ αBe allotropic transformation temperature of Be is 1270 °C.

Solubility of Be in Cu. The limits of the primary solid solution of (Cu) are well established through optical microscopy [32Bor, 52Abr], electrical conductivity [29Mas, 32Bor], lattice parameter [33Tan], and dilatometric [42Bor] measurements. As shown in Fig. 4, there is good agreement among the results of [29Mas], [32Bor], and [52Abr] above 500 °C, although below this temperature, the X-ray lattice parameter and dilatometry data of [33Tan] and [42Bor], respectively, are more reliable. In view of the excellent agreement among the results, the solvus above the eutectoid temperature is drawn through the data of [29Mas] and [52Abr] and below the eutectoid temperature through the data of [33Tan] and [42Bor]. The data of [33Tan] deviate considerably from the accepted values at higher temperatures. This trend may be inherent in the lattice parameter method and may be due to the change in composition of the powder specimen through contamination or through decomposition of one of the high-temperature phases during quenching [52Hum].

Decomposition of the β phase is difficult to suppress by quenching. Below the eutectoid temperature, these objections do not exist, and the lattice parameter method is apparently more accurate than the microscopic method, because the latter often fails to detect fine precipitates formed at lower temperatures and infers a wider single-phase field. Electrical conductivity measurements, although suitable for determination of solid-state phase boundaries at low temperatures, show scatter in the data of [29Mas] and [32Bor], which may be related to the lack of equilibrium in the structure. Experimental data on the solubility of Be in (Cu) are presented in Table 4.

Solubility of Cu in Be and in the Be-Rich Portion of the δ Phase. The solid solubility of Cu in (αBe) and (βBe) and in the Be-rich portion of the Be-Cu intermediate phase, δ, is

reduced in the presence of impurities. [50Kau] determined the former between 600 and 1100 °C by X-ray and metallographic methods using Be of 99.69 wt.% purity. [52Abr] determined the latter between 500 and 850 °C by metallography using Be of unspecified purity. [65Ham] and [68Jac] made accurate determinations of both boundaries between 1100 and 700 °C by electron probe microanalysis (EPMA) of diffusion couple sandwiches using zone-refined Be of 99.994 wt.% (99.998 at.%) and Cu of 99.999 wt.% purity. The results (Fig. 1 and 3 and Table 5) indicate further extensions of both single-phase fields, δ and (αBe). Thus, at the eutectoid temperature (1109 °C), the solubility of Cu in (αBe) reaches the maximum of 9.5 at.%, compared to the value 7.5 at.% at 1100 °C given by [50Kau]. Above 1109 °C, the boundaries of the (αBe) phase field are derived from the DTA measurements of [63Gel]. They also demonstrated that compared to Cu, metals like Ni, Co, Fe, and Cr have progressively lower solubility in Be. Because Cr, Fe, and Ni impurities were present in significant amounts (0.112 wt.% total) in the Be used by [50Kau], the reduced terminal solubility could be related partially to impurity effects.

[77Mye] extended the measurements for the solubility of Cu in (αBe) to lower temperatures, ranging from 750 to 320 °C, by enhancing the diffusivity in the samples through neon irradiation. The diffusion couples were prepared by ion implantation of Cu into single crystals of Be of 99.987 at.% purity, and the compositions were estimated by ion backscattering analysis. The results are presented in Fig. 1 and Table 5. The accepted results are taken from [65Ham] and [68Jac] and for the lower temperatures from [77Mye], in view of the high-purity metals and accurate measuring techniques used by these authors.

β/((Cu) + β) Boundary. This boundary was determined by optical microscopy by [29Mas], [32Bor], [41Iwa], and [52Abr]. The results are in good agreement. The accepted boundary is drawn through the data of [29Mas], [32Bor], and [41Iwa] (see Fig. 1).

β/(β + γ) and γ/(β + γ) Boundaries. Earlier works erroneously indicated that the β and γ phases were formed by two separate peritectic transformations and that the (β + γ) two-phase field terminated at the lower peritectic isotherm. [51Gru1] proposed a closed (β + γ) field that formed a two-phase field. This was confirmed by [52Abr] and [70Rau], who experimentally determined the gap boundaries. The accepted gap shown in Fig. 1 is taken from [70Rau] and has a triangular shape with a sharp maximum point at 45.8 at.% Be and 880 °C. See the section "β ⇄ γ Order-Disorder Transformation" for further details.

γ/(γ + δ) Boundary. This boundary is based on the metallographic data of [52Abr]. The resulting γ phase field is deficient in Be (by ~1 at.%) from the ideal equiatomic composition. The data of [65Ham] from high-purity Cu-Be diffusion couples indicate the boundary at slightly higher (0.4 to 0.8 at.%) than equiatomic Be composition. However, in view of the relatively lower accuracy of microprobe analysis at these compositions, the boundary given by [52Abr] is accepted in this evaluation.

γ/((Cu) + γ) Boundary. The studies of [41Iwa] suggest that this boundary shifts to higher Be content immediately below the eutectoid temperature (620 °C), thus narrowing the γ field considerably. The assessed boundary is tentatively shown by a dotted line.

δ/(γ + δ) Boundary. This boundary is drawn from the only available data [65Ham, 68Jac], which are based on high-purity Cu-Be diffusion couples that were equilibrated isothermally at different temperatures. The compositions were determined by EPMA.

β ⇄ (Cu) + γ Eutectoid Transformation Temperature. All determinations of this temperature made during cooling of the sample were uniformly low, regardless of whether they were based on thermal analysis (573 to 598 °C) [16Oes, 32Bor, 41Iwa, 42Los, 50Fil] or other methods (590 to 601 °C) [44Tho, 70Rau] (see Table 6). The corresponding temperatures measured during heating were always higher, regardless of whether they were based on thermal analysis (614 °C) [50Fil], electrical conductivity (618 °C) [44Tho], or isothermal decomposition methods (605 to 608 °C) [50Fil, 65Mor]. The existence of a temper-

Table 6 Reported β ⇄ α + γ Eutectoid Temperatures

Reference	Temperature, °C	Method	Thermal mode
[16Oes]	575 to 577	Thermal analysis	Cooling
[32Bor]	575	Thermal analysis	Cooling
[41Iwa]	573	Thermal analysis	Cooling
[42Los]	578	Thermal analysis	Cooling
[44Tho]	601	Electrical conductivity	Cooling
	618		Heating
[50Fil]	598	Thermal analysis	Cooling
	614		Heating
	608	Isothermal transformation	
[65Mor]	605 to 610	X-ray, microscopy	
[70Rau]	590	X-ray (disappearing phase method)	Average of heating and cooling
[71Shi2]	≥620	Reversion experiment	Heating
[74Auv]	580	DSC (a), X-ray	Heating (?)
[79Rio]	~620	DSC	Heating ≤40 °C/min
[82Gar]	614 to 624	X-ray (disappearing phase), TEM, SAD (b)	Heating from R.T., isothermal holding
[82Kal]	600, 597	DTA	Heating (3 K/min)
	583, 547		Cooling (3 K/min)

(a) DSC ≡ differential scanning calorimeter. (b) SAD ≡ selected area electron diffraction.

ature hysteresis of 16 to 20 °C between heating and cooling [44Tho, 50Fil, 70Rau] reported in these studies suggests that the reaction kinetics are very sluggish near the invariant temperature. This was also reported by [82Gar], who located the transformation temperature between 614 and 624 °C, based on isothermal phase disappearance studies of alloys (designated as high purity) at high temperatures by X-ray, supplemented by transmission electron microscopy (TEM), and select area electron diffraction (SAD) studies. Thus, the invariant temperature is apparently higher than previously indicated. However, the purity levels of the different alloys studied are not known. This fact, together with the difficulty in attaining equilibrium at the invariant temperature, makes the selection of the eutectoid temperature from the reported results difficult. The accepted temperature is taken tentatively from the highest reported temperature during heating, namely 620 °C [79Rio], which lies within the temperature limits of [82Gar].

$\beta \rightleftarrows$ (Cu) + γ Eutectoid Transformation. The β phase cannot be retained in the completely disordered state, regardless of the composition or the severity of the quenching rate [77Auv], which is contrary to the earlier reports of [50Fil]. The initial rate of decomposition is slower for hypoeutectoid (<31.5 at.% Be) alloys, because proeutectoid fcc (Cu) requires more atomic rearrangement to form from the bcc β phase. In contrast, the reaction rate is very rapid for hypereutectoid compositions, where the proeutectoid γ phase has the CsCl-type structure, which is a crystallographic derivative of the bcc structure [55Vis, 62Zak, 73Tad, 73Tya1, 73Tya2, 74Auv, 77Auv]. The decomposition of the hypereutectoid β phase proceeds as follows [73Tad, 73Tya1, 73Tya2, 74Auv, 74Gol, 77Auv]:

$$\beta \rightarrow \beta'' + \beta \rightarrow \gamma + \beta \rightarrow \gamma + (\mathrm{Cu})_T \rightarrow \gamma + (\mathrm{Cu})$$

The precipitation of the ordered γ phase from the β phase is preceded by the formation of the metastable ordered phase β'' of stoichiometry Cu_2Be, having a tetragonal structure [73Tya1, 73Tya2]. Superlattice reflections for this phase are observed in addition to those due to the γ phase [77Auv]. The formation of the metastable β'' phase was observed only after severe quenching, such as splat cooling [73Tya1, 77Auv]. During the early stage of formation of the γ phase, <001>satellite reflections were also observed near the fundamental spots, along with <001> striations in the electron micrograph [77Auv]. These phenomena indicate the formation of periodic modulations of the Cu concentration that result from the progressive rejection of excess Cu from γ. This produces fine Cu platelets on $\{001\}_\gamma$ planes [73Tad, 77Auv]. Eventually, this reaction leads to the formation of the transitional $(Cu)_T$ phase, which has a tetragonal structure. Depending on the quenching rate or annealing conditions of the quenched alloy, the transition from the metastable $(Cu)_T$ to equilibrium (Cu) proceeds through a series of intermediate stages of successive misorientations and variations in lattice parameters [73Tad, 77Auv].

$\beta \rightleftarrows \gamma$ Order-Disorder Transformation. [52Abr] determined the (β + γ) two-phase field by optical microscopy from the distribution of phases in specimens quenched from high temperatures. The results indicated an asymmetric two-phase field with a rounded top and a maximum temperature of 890 °C at 45.2 at.% Be, as shown in Fig. 5. [70Rau] refined the shape further, based on equilibrium phase distribution and phase disappearance studies, coupled with lattice parameter measurements by X-ray dif-

Fig. 5 Section of the Cu-Be Phase Diagram Showing Proposed Relationship Between Higher Order Transition and Two-Phase Field

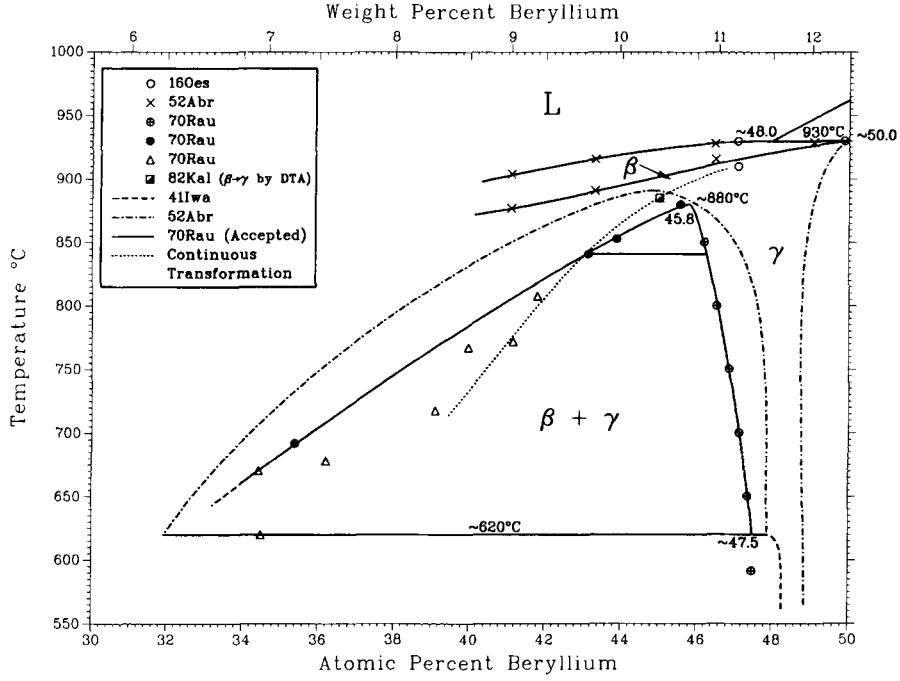

D.J. Chakrabarti, D.E. Laughlin and L.E. Tanner, 1987

fraction at high temperatures. The resultant phase field is markedly angular in shape with the maximum located at 880 °C and 45.8 at.% Be. Compared to the uncertainties of retaining the equilibrium distribution of phase mixtures from high temperatures in the quenched structure, as in the works of [52Abr], the *in situ* high-temperature measurements by [70Rau] are more reliable for the determination of the phase boundaries. However, the data of [70Rau] show considerable scatter at the $\beta/(\beta + \gamma)$ boundary. This may be due to the lack of equilibrium in the samples, particularly because these alloys are noted for sluggishness in reaching equilibrium. The authors did not report any specific measures to overcome this.

Above the maximum temperature, a continuous solid solution field between the β and γ phases was indicated by [52Abr]. This is, however, not possible, and a higher order transition boundary must exist in this region. This was indicated schematically by [70Rau]. However, the boundary of the continuous order-disorder transition at which the β and γ phases are indistinguishable (with respect to volume, entropy, or composition) was not determined. [70Rau] indicated that the schematic boundary passed through the maximum point, indicating that the latter is a tricritical point. (See [37Lan], [74Gri], [76All], [82All].) At such a point, the higher order transition ($A2 \rightleftarrows B2$) breaks into a first order transition below the maximum in the two-phase region. However, in the absence of experimental evidence, the position of the intersection of the $A2 \rightleftarrows B2$ higher order transition line with the two-phase field need not intersect at the maximum; more generally it intersects to one side, at a point called a critical end point [82All]. Indeed [82Kal] observed, by DSC heating, the $\beta \rightleftarrows \gamma$ transition for a 45 at.% Be alloy to be at 883 °C. This would put the intersection to the left of the maximum of the two-phase field. [78Ino] modeled the position of the higher-order transition line relative to the two-phase field in terms of the relative values of second neighbor exchange energy (positive) to first neighbor exchange energy (negative).

Within the two-phase $(\beta + \gamma)$ region, several sequences of phase transformation can be obtained. Above the extrapolated $\beta \rightleftarrows \gamma$ continuous transition boundary, the β phase is stable with respect to continuous ordering and metastable with respect to phase decomposition. Only nucleation and growth of the γ phase can occur. Below the extrapolated continuous transition boundary, the β phase is unstable with respect to continuous ordering. After the β phase orders homogeneously to a phase with the same symmetry as γ but the composition of the original β, it becomes unstable with respect to phase decomposition. [76All] termed this phenomenon the "conditional spinodal" (see also [82Sof]).

Continuous vs Discontinuous Transformation. Depending on the composition and the thermomechanical history, both continuous (i.e., uniformly nucleated) [52Gei] and discontinuous (i.e., heterogeneously formed) [48Guy] modes of transformation of the supersaturated solid solution of Be in (Cu) have been observed. Studies are reported in terms of the kinetic variables [60Ent, 78Tsu] and various metallurgical factors governing these reactions, such as the effects of cold work [60Ent, 71Kre], solutionizing temperature [75Rak, 82Ale], aging temperature [74Bon2], quenching sequence [82Ale], atomic size difference [61Boh], or precipitate size and additions of third elements, such as Co [49Bec, 59Tho, 66Mur, 68Mur1, 74Bon2, 80Tsu], Ce [80Bau], and other elements [83Mik]. In view of the importance of these factors in restricting discontinuous transformations to develop strong engineering alloys, a short summary from the above findings is presented below. The nose of the *TTT* curve for the discontinuous reaction shifts to higher temperatures and to shorter times with increasing Be content and to longer times with increasing grain size of the (Cu) phase. The reaction can be inhibited by deformation, or by large random precipitates formed prior to or during the process. Quenching from high solutionizing temperatures is beneficial, as it aids in the growth of continuous precipitates by thermal diffusion due to excess vacancies. Both Co and Ce are effective in suppressing the cellular reaction, Ce being more effective for higher aging temperatures. The formation of cuboidal precipitates rich in Co [60Ent, 78Wil] or, alternatively, in Ce [80Bau] is believed to be the responsible mechanism, because preferential segregation of these elements to the grain boundaries has not been observed.

Effect of Pressure on Solid Solubility. No studies have been reported on the Cu-Be binary alloys under pressure. [61Phi] made such studies on the commercial Cu–2.1 wt.% Be–0.4 wt.% Ni alloy. Application of pressure at 70 to 76 kbar reduced the solubility of Be in Cu by half at 825 °C (solutionizing temperature) and by one third at 396 °C (aging temperature).

Metastable Phases

The low-temperature decomposition of the supersaturated solid solution of Be in (Cu) (or α) passes through several intermediate metastable phases prior to the formation of the equilibrium precipitate phase. The sequence of phase separation is as follows*:

Supersaturated solid solution:

$$\alpha_s \rightarrow \alpha + \text{GP zone} \rightarrow \alpha + \gamma'' \rightarrow \alpha + \gamma' \rightarrow \alpha + \gamma$$

The details of these phase transformation sequences and the associated metastable phases are reviewed in [80Rio].

GP Zone. Studies using X-ray [43Gui, 48Guy, 51Gru1, 51Gru2, 64Tya1, 64Tya2, 66Tya], electron diffraction [63Arm, 63Tan, 65Nak, 65Pfe, 66Tan, 67Sor, 69Wil, 71Shi1, 71Yam, 73Phi, 74Bon1, 80Rio], and TEM [66Tan, 67Sor] indicated that the GP zones are thin, essentially coherent monolayers of Be atoms, segregated parallel to the {100} planes of the matrix phase. A precursor to the plate-like GP zones was observed by [73Phi], [74Bon1], and [80Rio] and [86Koo]. [80Rio] described the precursor as "equiaxed" Be clusters, and [86Koo] described the precursor of "ellipsoidal" Be clusters.

γ'' Phase. X-ray [52Gei] and electron diffraction studies [69Yam, 71Shi1, 73Phi, 80Rio] attributed the γ'' phase to evolve from the "piling up" of GP zones with habit planes parallel to the {100} planes of the matrix α phase [65Pfe, 68Mur2, 69Yam, 73Phi, 80Rio] and coherent with them. Two different orientation relationships are proposed by [52Gei] and [71Shi1], respectively. Also see [80Rio] for a discussion of this topic.

* To conform with literature usage in stable and metastable phase transformations, (Cu) phase is represented by α in this section.

Fig. 6 Cu-Be Metastable Solvi

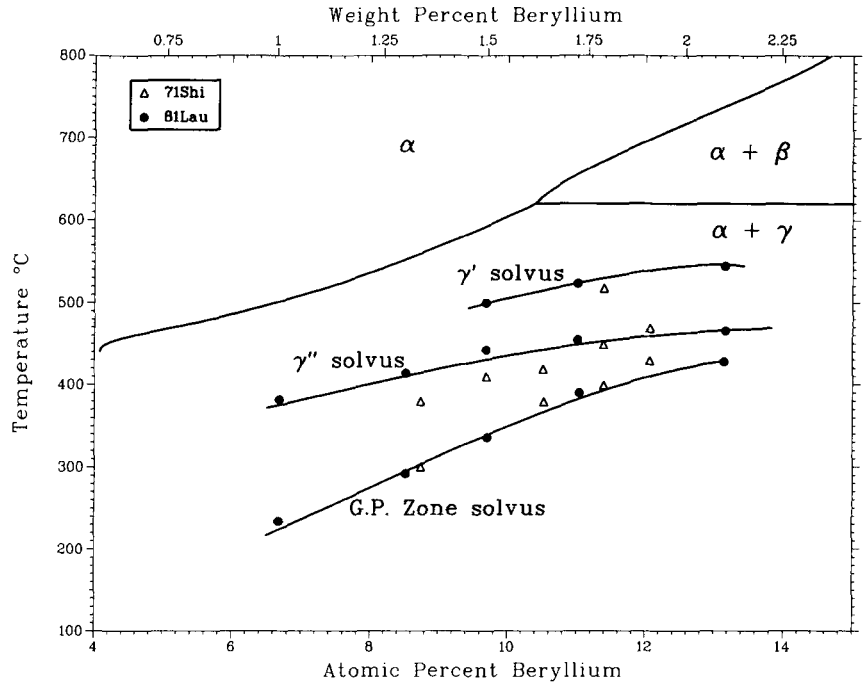

D.J. Chakrabarti, D.E. Laughlin and L.E. Tanner, 1987.

γ' Phase. The transition from γ'' to γ' metastable state has been studied by electron diffraction [71Shi1, 74Bon1]. Whether the γ'' phase undergoes dissolution [71Sho2], or transforms continuously to γ' phase is not known. The orientation relationships for the γ' platelets including the transitional stages are discussed in [52Gei, 65Nak, 69Wil, 71Shi1, 71Yam], [80Rio]. Crystal structure and lattice parameter measurements are reported in [51Gru1], [52Gei], [63Arm], [65Nak], [65Pfe], [66Hen], [71Shi1], [71Yam], [74Bon1], [79Bab], and [80Rio].

γ Phase. The continuous precipitation of γ within the α grains was studied by [60Ent, 71Shi1, 78Tsu]. Matrix orientation relationships were reported in [48Guy, 52Gei, 80Rio]. Striation markings in micrographs similar to those observed during GP zone formation were observed by [71Shi1]. Pretransformational modulation of shear strains and the associated martensite type of transformation aspects were reported in [59Blo, 66Tan, 74Tya1, 74Tya2, 81Sva, 82Tan].

A metastable ordered phase of stoichiometry Cu_2Be, designated β'', has been observed to form as an intermediate product during the formation of γ from the β phase. Likewise, the formation of the equilibrium α phase from the β phase is preceded by the formation of the metastable phase, α_T which undergoes successive stages of modification prior to transforming into the α phase [73Tad, 73Tya1, 77Auv].

[80Gie] studied the effect of rapid solidification on metastable phase equilibria in the Cu-Be system. The Cu-rich boundary of β was found to extend to ~19 at.% Be (as compared to equilibrium 23.5 at.%), and the CsCl-type ordered structure corresponding to the γ phase was observed in quenched, off-stoichiometric alloys with 32 at.% Be.

Metastable Solvi. Reversion phenomenon was studied by the electrical resistivity [51Gru1] and hardness methods [69Mis, 71Shi2]. [71Shi2] and [81Lau] delineated the metastable solvi for the GP zone, γ'', and γ' phases, by reversion experiments in conjunction with TEM metallography. The resultant solvi are presented in Fig. 6. For details, see [81Lau].

Crystal Structures and Lattice Parameters

The crystal structures and the accepted lattice parameters of the Cu-Be equilibrium and metastable phases are presented in Tables 7 and 8, respectively. The experimental lattice parameters for fcc (Cu) are presented in Table 9. [33Tan] observed that the lattice parameter of (Cu) varied approximately linearly with both composition and temperature and that it increased with decreasing Be content, reaching the maximum at pure Cu. Thus, alloys quenched from solutionizing temperatures, being supersaturated in Be, have lower lattice parameter values compared to alloys that are subsequently aged [29Dah, 65Nak]. A broadening of X-ray diffraction lines with the onset of γ' precipitation from the supersaturated solid solution and a progressive increase of lattice parameter from 0.3584 nm in the quenched condition to 0.3612 nm in the aged condition was obtained by [65Nak], with a 2 wt.% Cu-Be alloy. The broadening apparently arises from superposition of lines from (Cu) with varying compositions and lattice parameters during aging. On precipitation of the γ phase, the X-ray lines become sharper, and the lattice parameter levels off to a constant value as the composition reaches equilibrium. The lattice parameter did not show any notable change during GP zone formation.

Table 7 Cu-Be Crystal Structure Data

Phase	Composition, at.% Be	Pearson symbol	Space group	Strukturbericht designation	Prototype
(Cu)	0 to 16.5 at 866 °C	*cF*4	*Fm3m*	*A*1	Cu
β	24.5 to 43.5 at 850 °C	*cI*2	*Im3m*	*A*2	W
γ	46.2 to 49 at 850 °C	*cP*2	*Pm3m*	*B*2	CsCl
δ	$Cu_{1-x}Be_{2+x}$	*cF*24	*Fd3m*	*C*15	$MgCu_2$
(βBe)	~82 to 90 at 1200 °C	*cI*2	*Im3m*	*A*2	W
(αBe)	90.5 to 100	*hP*2	$P6_3/mmc$	*A*3	Mg
Metastable phases					
$(Cu)_T$	...	(a)	...	...	...
β''	66.67	(a)	...	...	Cu_2Be
γ''	...	(a)	...	...	...
γ'	...	(a)	...	...	...
δ'	75	(b)	...	...	$CuZn_3$

(a) Tetragonal. (b) Hexagonal.

Table 8 Cu-Be Lattice Parameter Data

Phase	Approximate composition, at.% Be	Temperature, °C	Lattice parameters, nm *a*	*b*	*c*	Comments	Reference
(Cu)	0 to 16.5	866	0.36147	...	...	At 18 °C, 0% Be	[Landolt]
			0.3612	...	...	(a)	[29Dah, 65Nak]
β	24.5 to 43.5	850	0.281	...	...	(b)	[74Auv]
γ	46.2 to 49	850	0.270	...	...	(b)	[43Gui, 52Gei, 63Pri, 71Shi1, 71Yam, 74Auv, 80Rio]
δ	$Cu_{1-x}Be_{2+x}$	...	0.5952	...	...	(c)	[35Mis, 42Los]
			0.5899	...	...	At $CuBe_3$ (x = 0.25)	[42Los]
(βBe)	~82 to 90	1200	0.25515	...	...	(d)	[61Amo]
(αBe)	90.5 to 100	...	0.22858 ± 0.00002	...	0.35843 ± 0.00003	(e)	[63Mac]
Metastable phases							
$(Cu)_T$	...	...	0.375	...	0.326	(f)	[73Tad, 74Auv]
β''	66.67	...	0.271	...	0.87	...	[77Auv]
γ''	...	...	$a/2$ = 0.253	0.253	0.29	...	[71Shi1]
γ'	...	...	0.270	0.270	0.256	...	[80Rio]
δ'	75	...	0.2557 ± 0.0003	...	0.4179 ± 0.0003	...	[66Mag, 69Pat]

(a) 12.6 at.% Be alloy quenched from 800 to 810 °C and aged at 350 °C for 5 h [29Dah], or aged at 150 to 400 °C up to 250 h [65Nak]. (b) 32 at.% Be alloy (prepared from 99.99% Be and OFHC Cu) at 750 °C [74Auv]. (c) At $CuBe_2$ (x = 0) composition (x varies from −0.071 at 930 °C to 0.455 at 1090 °C. (d) 99.97% Be (0.01% O, <0.02% C) at 1254 °C. (e) 99.9% purity vacuum distilled Be (250 ppm O) at 20.5 °C. (f) On 33.4 at.% Be alloy quenched from 820 °C in 10% aqueous NaOH at 0 °C; data from [73Tad]. a = 0.382 nm, c/a = 0.87, according to [74Auv] for quenched 31 and 39.5 at.% Be alloys.

The lattice parameter values of the bcc β phase and the CsCl-type ordered cubic γ phases are presented in Tables 10 and 11, respectively. The results exhibit reasonable agreement.

The solubility range of the δ phase (Fig.1) encompasses the compositions between 66.7 and 75 at.% Be. Thermal analysis plots indicated an anomalous change in slope at 75 at.% Be [16Oes, 32Bor, 42Los]. X-ray analysis, however, showed that the cubic $MgCu_2$-type structure was present over the entire composition range with a change in lattice parameter from 0.5952 nm at 66.7 at.% Be to 0.5899 nm at 75 at.% Be [42Los]. However, [66Mag] and [69Pat] reported a cph $CuZn_3$-type structure in the X-ray pattern at 75 at.% Be. The samples were prepared by thermodiffusion of Be powder or Be coating on copper lamina or of a mixture of Cu and Be powder in the ratio of 1 to 3 at 800 °C under hydrogen and chlorine atmosphere.

The same studies also revealed a $MgCu_2$-type cubic phase at 66.7 at.% Be composition with the lattice parameter of a = 0.5969 ± 0.0002 nm [69Pat]. This would suggest that two distinct compounds, namely $CuBe_2$ and $CuBe_3$, occur in place of the homogeneous single phase δ. However, this would entail the occurrence of two-phase fields and temperature invariants between 930 and ~1215 °C, none of which has been observed experimentally. This fact, together with the X-ray findings of a homogeneous single phase by [42Los], preclude the above two-compound hypothesis. The $CuZn_3$-type structure obtained on thermodiffusion treatment of CuBe alloys is believed to correspond to a metastable equilibrium. This possibility is further supported by the report of a phase equilibrium between fcc (Cu) and the cph $CuBe_3$ phases observed by [66Mag] that does not follow the equilibrium phase relationships in Fig. 1. Accordingly, the δ phase is accepted as having the cubic $MgCu_2$-type structure with a Cu-deficient composition over much of the phase field, forming a defect compound. The formula of the δ phase can be represented as $Cu_{1-x}Be_{2+x}$, with x varying from −0.071 to 0.45.

(αBe) has a cph structure and undergoes an allotropic transformation to bcc (βBe) at higher temperature. This

Table 9 Lattice Parameter of (Cu) Phase

Reference	Lattice parameter, nm	Comments
[29Dah]	0.3564	15.3 at.% Be, quenched from 810 °C
	0.3596	15.3 at.% Be, aged at 350 °C, 5 h
	0.3575	12.6 at.% Be, quenched from 810 °C
	0.3612	12.6 at.% Be, aged at 350 °C, 5 h
[33Tan]	0.36080	0 at.% Be, quenched from 810 to 850 °C
	0.35993	2.8 at.% Be, quenched from 810 to 850 °C
	0.35902	6.1 at.% Be, quenched from 810 to 850 °C
	0.35771	10.2 at.% Be, quenched from 810 to 850 °C
	0.35662	13.1 at.% Be, quenched from 810 to 850 °C
[33Tan] (a)	0.35674	800 °C, 8 h
	0.35714	700 °C, 12 h
	0.35776	600 °C, 24 h
	0.35874	500 °C, 48 h
	0.35985	400 °C, 96 h
	0.3604	250 °C, 24 h (14.51 at.% Be)
[35Kos]	0.362	At 570 °C, 35.36 at.% Be
[55Vis]	0.359	31 at.% Be, quenched from 750 °C
[65Nak]	0.3584	12.6 at.% Be, quenched state
	0.3612	12.6 at.% Be, aged 150 to 400 °C, 250 h
[66Mag]	0.3615	Sample from thermodiffusion of Be powder and Cu lamina at 800 °C
[73Tad]	0.357	33.4 at.% Be, aged above 300 °C

Note: Results of [65Nak] and [73Tad] are based on electron diffraction; the remainder are based on X-ray studies.
(a) Results are given for 14.67 at.% Be alloy at 20 °C, following heat treatment at temperature and times indicated.

Table 10 Lattice Parameter of the β Phase

Reference	Lattice parameter, nm	Comments
[35Kos]	0.279	35.4 at.% Be at 570 °C
[55Vis]	0.278	31.0 at.% Be, quenched from 750 °C
[74Auv]	0.279	32.0 at.% Be (from 99.99% Be + OFHC Cu) at eutectoid temperature
	0.281	32.0 at.% Be at 750 °C

Table 11 Lattice Parameter of the γ Phase

Reference	Lattice parameter, nm	Comments
[29Dah]	0.2689 to 0.2705	15.3 at.% Be, aged 350 °C?
[35Kos]	0.272	35.4 at.% Be at 570 °C
[35Mis]	0.27	50.23 at.% Be
[43Gui]	0.27	...
[63Pri]	0.271	...
[65Nak]	0.2689	12.6 at.% Be, aged at 400 °C, 100 h
[69Pat]	0.2702 ± 0.0003	Sample from thermodiffusion of Be powder in Cu lamina at 800 °C
[71Shi1]	0.271	...
[71Yam]	0.270	9.16 at.% Be, aged at 300 °C, 20 h
[73Tad]	0.271	33.4 at.% Be, quenched from 820 °C
[74Auv]	0.270	32.0 at.% Be, slow cooling from 800 °C
	0.272	32.0 at.% Be, at 580 °C

Note: The results of [29Dah], [35Kos], [35Mis], and [43Gui] are based on X-ray; all other results are based on electron diffraction.

was observed by [59Mar] with thermal and X-ray techniques on 99.4 wt.% pure Be and by [61Amo] with electrical resistivity and X-ray at high temperatures on 99.97% pure Be. The lattice parameter values for the two allotropic forms of Be presented in Table 8 are for elemental Be, because data for alloys are not available.

Thermodynamics

Partial molar quantities for solid alloys in the concentration range 2.1 to 99.5 at.% Be were determined by [62Anf] by the electrochemical cell method (emf). Select values of both partial and integral quantities versus composition at 1073 K are presented in [Hultgren, B]. Improved measurements were made by [68Gav], also by the emf method, between 1000 and 1135 K on alloys up to 35 at.% Be, that include the (Cu) solid solution region. The total impurity content in the alloys was quoted as 0.4%. The derived relative partial molar heat of mixing for Be, ΔH_{Be}, and for Cu, ΔH_{Cu} (calculated from that of ΔH_{Be} applying the Gibbs-Duhem relation), and the respective activity coefficients as functions of composition at 1000 K are presented in Table 12 after [68Gav]. The results in conjunction with those in [Hultgren, B] show that both the relative partial molar heat of mixing and the relative integral molar Gibbs energy values for the terminal solid solutions at either end are negative.

The activity coefficient of Cu in infinite dilution in liquid Be at 1623 K was determined by [68Bie] as:

$$\gamma^{\infty}_{Cu(Be)} = 0.92$$

[84Kau] derived analytic models for the different phases in the Cu-Be system, based on the lattice stability values for Be and Cu [70Kau], combined with the limited thermodynamic [Hultgren, B] and phase diagram data. The calculated phase diagram is at variance with the experimental one; in particular, it fails to reproduce the (β + γ) two-phase field and denotes the γ and δ phases as line compounds.

Cited References

***16Oes:** G. Osterheld, "On the Melting Point and Heat of Fusion of Cu-Be Alloys," *Z. Anorg. Chem., 97*, 13-27 (1916) in German. (Equi Diagram; Experimental; #)

29Dah: O. Dahl, E. Holm, and G. Masing, "X-Ray Investigation of Be-Cu Alloys," *Wiss. Veroffentl. Siemens-Konzern, 8,* 154-186 (1929) in German. (Crys Structure; Experimental)

***29Mas:** G. Masing and O. Dahl, "On Constitution of Cu-Be Alloys," *Wiss. Veroffentl. Siemens-Konzern, 8,* 94-100 (1929) in German. (Equi Diagram; Experimental; #)

***32Bor:** H. Borchers, "Investigation of Cu-Be System," *Metallwirtschaft, 11*, 317-321, 329-330 (1932) in German. (Equi Diagram; Experimental; #)

***33Tan:** H. Tanimura and G. Wassermann, "On Cu-Be System," *Z. Metallkd., 25*, 179-181 (1933) in German (Equi Diagram, Crys Structure; Experimental; #)

35Kos: G. F. Kossolapow and A.K. Trapesnikow, "X-Ray Analysis of β-Phase in Cu-Be and Al-Zn Alloys at High Temperatures," *Metallwirtschaft, 14*, 45 (1935) in German. (Crys Structure; Experimental)

35Mis: L. Misch, "Structure of Intermetallic Compounds of Be with Cu, Ni and Fe," *Z. Phys. Chem. B, 29*, 42-58 (1935) in German, quoted in [Hansen]; *Chem. Abstr.*, Vol. 29, 5715 (1935). (Crys Structure; Experimental)

Table 12 Thermodynamic Properties of Solid Cu-Be Alloys at 1000 K

Atomic fraction of Be (N_{Be})	Activity coefficient of Be ($lg\gamma_{Be}$)	Activity coefficient of Cu ($lg\gamma_{Cu}$)	Partial molar heat of mixing of Be (ΔH_{Be}) kJ/mol	Partial molar heat of mixing of Cu(ΔH_{Cu}) kJ/mol
0	−3.77	0	280.75	0
0.01	−3.46	−0.001	254.81	0.13
0.02	−3.14	−0.006	229.28	0.50
0.03	−2.83	−0.014	204.18	1.17
0.04	−2.53	−0.025	179.91	2.05
0.05	−2.21	−0.040	155.23	3.22
0.06	−1.92	−0.057	130.54	4.60
0.07	−1.62	−0.078	106.27	6.28
0.08	−1.32	−0.102	82.01	8.37
0.09	−1.03	−0.129	58.99	10.46
0.10	−0.74	−0.159	38.07	12.55
0.11	−0.50	−0.187	23.85	14.23
0.12	−0.32	−0.211	14.64	15.48
0.13	−0.19	−0.229	7.95	16.53
0.288	−0.542	−0.142	49.37	6.28
0.30	−0.517	−0.142	43.51	8.79
0.31	−0.490	−0.154	39.96	10.25
0.32	−0.465	−0.165	37.03	11.51
0.33	−0.435	−0.180	35.15	12.55
0.34	−0.407	−0.194	33.68	13.18
0.35	−0.374	−0.211	33.05	13.60

From [68Gav].

37Lan: L.D. Landau, *Phys. Z. Sowjetunion.*, *11*, 26 (1937), quoted in [74Gri]. (Equi Diagram; Theory)

41Iwa: K. Iwase and M. Okamoto, "Equilibrium Diagrams of Be-Cu and Be-Ni-Cu Systems," *Nippon Kinzoku Gakkai-Shi (J. Jpn. Inst. Met.)*, *5*, 82-84 (1941) in Japanese. (Equi Diagram; Experimental; #)

***42Bor:** H. Borchers and H.J. Otto, "Study of $\alpha/(\alpha+\gamma)$ Boundary in Cu-Be System," *Metallwirtschaft*, *21*, 215-217 (1942) in German. (Equi Diagram; Experimental; #)

42Los: L. Losana and G. Venturello, *Alluminio*, *11*, 8-16 (1942) quoted in [Hansen]; *Chem. Abstr.*, *37*, 5004 (1943). (Equi Diagram, Crys Structure; Experimental)

43Gui: A. Guinier and P. Jacquet, "On Age-Hardening of Cu-Be Alloys," *Compt. Rend.*, *217*(1), 22-24 (1943); *Rev. Met.*, *41*, 1-16 (1944) both in French. (Meta Phases, Crys Structure; Experimental)

44Tho: H. Thomas, "Chances of Volume and Electrical Resistivity on Heat Treatment of Cu-Be Alloys," *Z. Metallkd.*, *36*, 136-140 (1944). (Equi Diagram; Experimental)

48Guy: A.G. Guy, C.S. Barrett, and R.F. Mehl, "Mechanism of Precipitation in Alloys of Be in Cu," *Trans. AIME*, *175*, 216-238 (1948). (Meta Phases; Experimental)

49Bec: P.A. Beck, "Some Factors Affecting Rate of Precipitation Hardening in Cu-Be Alloys," *J. Appl. Phys.*, *20*, 666-668 (1949). (Equi Diagram; Experimental)

49Ray: G.V. Raynor, "Equilibrium Diagram of System Be-Cu," *Annotated Equilibrium Diagrams*, No. 7, Inst. Met., London (1949). (Equi Diagram, Crys Structure; Review)

***50Fil:** R.F. Fillnow and D.J. Mack, "Isothermal Transformation of Eutectoid Be Bronze," *Trans. AIME*, *188*, 1229-1236 (1950). (Equi Diagram; Experimental)

50Kau: A.R. Kaufmann, P. Gordon, and D.W. Lillie, "Metallurgy of Be," *Trans. ASM*, *42*, 785-844 (1950). (Equi Diagram; Experimental)

51Gru1: W. Gruhl and G. Wassermann, "On Precipitation Process in Cu-Be Alloys," *Metall.*, *5*, 93-98 (1951); *Metall.*, *5*, 141-145 (1951) in German. (Meta Phases, Crys Structure; Experimental)

51Gru2: W. Gruhl, "About Reformation Phenomena in Cu-Be," *Metall.*, *5*, 231-238 (1951) in German. (Meta Phases, Crys Structure; Experimental)

***52Abr:** N.Kh. Abrikosov, "Study of Cu-Be System," *Izv. Sekt. Fiz. Khim. Anal., Akad. Nauk SSSR*, *21*, 101-115 (1952) in Russian. (Equi Diagram; Experimental; #)

***52Gei:** A.H. Geisler, J.H. Mallery, and F.E. Steigert, "On Mechanism of Precipitation in Cu-Be Alloys," *Trans. AIME*, *194*, 307-316 (1952). (Meta Phases, Crys Structure; Experimental)

52Hum: W. Hume-Rothery, J.W. Christian, and W.B. Pearson, *Metallurgical Equilibrium Diagrams*, Inst. Phys., London, 184, 210-211 (1952). (Equi Diagram; Review)

55Vis: A. Viswanathan, "On Eutectoid Transformation of a Cu-6% Be Alloy," *Compt. Rend.*, *240*, 626-628 (1955) in French. (Equi Diagram, Crys Structure; Experimental)

59Blo: R.J. Block and G.H. Kehl, "Resistivity Measurement on Eutectoid Be-Cu," *Trans. AIME*, *215*, 878-879 (1959). (Equi Diagram; Experimental)

59Mar: A.J. Martin and A. Moore, "Structure of Be with Particular Reference to Temperature Above 1200 °C," *J. Less-Common Met.*, *1*, 85-93 (1959). (Equi Diagram; Experimental)

59Tho: H. Thomas and U. Wilke-Dorfurt, "Influence of Additions on Hardening of Cu-Be Alloys," *Z. Metallkd.*, *50*, 466-472 (1959) in German. (Equi Diagram; Experimental)

60Ent: A.R. Entwisle and J.K. Wynn, "Precipitation in Commercial Cu-Be Alloys," *J. Inst. Met.*, *89*, 24-29 (1960). (Equi Diagram; Experimental)

61Amo: V.M. Amonenko, V.Ye. Ivanov, G.F. Tikhinskii, V.A. Finkels, and I.V. Shpagin, "High Temperature Polymorphism of Be," *Fiz. Metal. Metalloved.*, *12*, 865-871 (1961) in Russian; TR: *Phys. Met. Metallogr.*, *12*(6), 77-82 (1961). (Crys Structure; Experimental)

61Boh: H. Bohm, "On Precipitation Behavior of Binary Cu Alloys and its Influence due to Alloying," *Z. Metallkd.*, *52*(9), 564-571 (1961) in German. (Equi Diagram; Experimental)

61Phi: V.A. Phillips, "Effect of Pressure on Age Hardening Characteristics of Cu-Be-Ni Alloy," *Acta Metall.*, *9*, 216-224 (1961). (Pressure; Experimental)

62Anf: A.I. Afinogenov, M.P. Smirnov, N.G. Ilushchenko, and G.I. Belyaeva, *Trudi in-ta Elektrokhim. Akad. Nauk SSSR Ural'sk. Filial*, *3*, 83-100 (1962) in Russian. (Thermo; Experimental)

62Zak: M.I. Zakharova and Ye.M. Amosov, "β Phase Transformations in Cu-Be System," *Fiz. Metal. Metalloved*, *14*, 559-563 (1962) in Russian; TR: *Phys. Met. Metallogr.*, *14*(4), 71-76 (1962). (Equi Diagram, Crys Structure; Experimental)

63Arm: W.K. Armitage, Ph.D. thesis, University of Leeds (1963). (Meta Phases; Experimental)

*63Gel: S.H. Gelles, J.J. Pickett, E.D. Levine, and W.B. Nowak, "Stability of Hgh Temperature Phase in Be and Be Alloys," Proc. Conf. on *The Metallurgy of Beryllium*, Inst. Met., London, No. 28, 588-600 (1963). (Equi Diagram; Experimental; #)

63Mac: K.J.H. Mackay and N.A. Hill, "Lattice Parameter and Hardness Measurement on High Purity Be," *J. Nucl. Mater.*, *8*(2), 263-264 (1963). (Crys Structure; Experimental)

63Pri: R.J. Price and A. Kelly, "Deformation of Age Hardened Crystals of Cu-1.8 wt.% Be," *Acta Metall.*, *11*, 915-922 (1963). (Meta Phases; Experimental)

63Tan: K. Tanaka, M. Mannami, K. Izumi, and K. Marukawa, "Structure of GP Zone in Cu-2% Be Alloy," *Acta Metall.*, *11*, 79-81 (1963). (Meta Phases; Experimental)

64Tya1: Yu.D. Tyapkin, "Monoclinic Distortion of Cubic Lattice in Aging of Ni-Be and Cu-Be Alloys," *Dokl. AN SSSR, 154*, 578-581 (1964) in Russian; TR: *Sov. Phys.-Dokl.*, *9*, 95-98 (1964). (Meta Phases; Experimental)

64Tya2: Yu.D. Tyapkin and A.V. Gavrilova, "Study of Anomalous Scattering of X-Rays in Microscopical Single Crystals of Alloys. First Stage of Aging in Ni-Be and Cu-Be Alloys," *Kristallografiya*, *9*, 213-218 (1964) in Russian; TR: *Sov. Phys. Crystallogr.*, *9*, 166-171 (1964). (Meta Phases; Experimental)

*65Ham: M.L. Hammond, A.T. Davinroy, and M.I. Jacobson, "Be-Rich End of Five Binary Systems," Tech. Rept. AFML-TR-65-223, 1-77 (1965). (Equi Diagram; Experimental; #)

65Mor: T. Morinaga, T. Goto, T. Takahashi, and I. Mamiya, "Phase Transformation of Hypo-Eutectoid Cu-Be Alloy during High Temperature Tempering," *J. Jpn. Inst. Met.*, *29*, 787-793 (1965) in Japanese. (Equi Diagram; Experimental)

65Nak: M. Nakagawa, "Precipitation of Cu-Be Compounds from Supersaturated Solid Solution of Cu-2% Be Alloy," *Jpn. J. Appl. Phys.*, *4*, 760-766 (1965). (Meta Phases, Crys Structure; Experimental)

*65Pfe: I. Pfeiffer, "Electron Microscopic Investigation of Age-Hardening of Cu-Be Alloys," *Z. Metallkd.*, *56*, 465-469 (1965) in German. (Meta Phases; Experimental)

66Hen: Z. Henmi and T. Nagai, "On Mechanism of Precipitation in Cu-2 wt.% Be Alloy," *J. Jpn. Inst. Met.*, *30*, 400-406 (1966). (Meta Phases; Experimental)

66Mag: L.S. Magomedova and G.V. Davydov, "The Compound $CuBe_3$," *Uch. Zap. Chuv. Gos. Pedagog. Inst.*, *5*, 39-42 (1966) in Russian; *Chem. Abstr.*, 68-90650t (1968). (Crys Structure; Experimental)

66Mur: Y. Murakami, H. Yoshida, T. Kawashima, and S. Yamamoto, "Effect of Additional Elements on Discontinuous Precipitation in Cu-Be Alloys," *J. Jpn. Inst. Met.*, *30*, 508-514 (1966). (Equi Diagram; Experimental)

*66Tan: L.E. Tanner, "Diffraction Contrast from Elastic Shear Strains due to Coherent Phases," *Philos. Mag.*, *14*(127), 111-130 (1966). (Meta Phases; Experimental)

*66Tya: Yu.D. Tyapkin, "Nature of Changes in Crystal Structure of Ni-Be and Cu-Be Alloys in First Stage of Aging," *Kristallografiya*, *10*(4), 501-508 (1965) in Russian; TR: *Sov. Phys. Crystallogr.*, *10*(4), 418-424 (1966). (Meta Phases, Crys Structure; Experimental)

67Sor: L.M. Sorokin, "Electron Microscopic Investigation of Initial Stages in the Decompostion of Supersaturated Cu-2 at.% Be Solid Solution," *Sov. Phys.—Solid State*, *8*, 2820-2828 (1967); quoted in [74Bon1]. (Meta Phases, Crys Structure; Experimental)

68Bie: G. Bienvenu, C. Potard, B. Schaub, and P. Desre, "Determination of Thermodynamic Activity of Fe, Ni, Al and Cu in Dilute Solutions in Liquid Be," Proc. Symp. *Thermodynamics of Nuclear Materials. 1967*, Intl. Atomic Energy Agency, Vienna, (1968). (Thermo; Experimental)

*68Gav: L.G. Gavrilenko, V.I. Malkin, B.M. Mogutnov, and V.V. Pokidyshev, "Aging Peculiarities due to Thermodynamic Properties of Cu-Be Alloys," *Fiz. Metal. Metalloved.*, *25*(3), 469-472 (1968); TR: *Phys. Met. Metallogr.*, *25*(3), 92-96 (1968).

68Jac: M.I. Jacobson and M.L. Hammond, "Solid Solubilities of Ag, Al, Cr, Cu and Fe in Zone-Refined Be," *Trans. AIME*, *242*, 1385-1391 (1968). (Equi Diagram; Experimental; #)

68Mur1: Y. Murakami, H. Yoshida, and S. Yamamoto, "On Aging Characteristics of Cu-2 wt.% Be Alloys with or without Additional Elements," *Trans. Jpn. Inst. Met.*, *9*, 11-18 (1968). (Meta Phases; Experimental)

68Mur2: Y. Murakami, O. Kawano, and S. Yamamoto, Presented at Spring Meeting of JIM, Tokyo, April 4 (1968); quoted in Z. Henmi and T. Nagai, "Mechanism of Precipitation Hardening in Cu-Be Alloys," *Trans. Jpn. Inst. Met.*, *10*, 166-173 (1969). (Meta Phases; Experimental)

*69Mis: Y. Mishima, T. Okubo, and R. Shiromizu, "Aging, Reversion and Reaging of Cu-Be Alloys," *Trans. Jpn. Inst. Met.*, *10*, 73-80 (1969). (Meta Phases; Experimental)

69Pat: L.S. Patskhverova, "Nature of δ Phase in Cu-Be System," *Izv. V.U.Z., Fiz.*, *12*(5), 122-123 (1969) in Russian; TR: *Sov. Phys. J.*, *12*(5), 646-647 (1969). (Equi Diagram, Crys Structure; Experimental)

69Wil: P. Wilkes and M.M. Jackson, "Electron Microscope Study of Precipitation in Cu-Be Alloys," *Met. Sci. J.*, *3*, 130-133 (1969). (Meta Phases; Experimental)

69Yam: S. Yamamoto and Y. Murakami, Mem. Fac. Eng. (Kyoto University), *31*, 576 (1969); quoted in [71Yam]. (Meta Phases; Experimental)

70Kau: L. Kaufman and H. Bernstein, *Computer Calculation of Phase Diagrams*, Academic Press, New York, 185 (1970). (Thermo; Theory)

*70Rau: R. Rautioaho and E. Suoninen, "Study of Ordering in Cu-Be β Phase," *Phys. Status Solidi (a)*, *2*, 493-496 (1970). (Equi Diagram; Experimental; #)

71Kre: H. Kreye, "Influence of Prior Cold Work on Discontinuous Precipitation in Cu-2 wt.% Be," *Z. Metallkd.*, *62*(7), 556-562 (1971). (Equi Diagram; Experimental)

*71Shi1: K. Shimizu, Y. Mikami, H. Mitani, and K. Otsuka, "Electron Microscopy Study of Precipitation Processes in Cu-2 wt.% Be Alloy," *Trans. Jpn. Inst. Met.*, *12*, 206-213 (1971). (Meta Phases, Crys Structure; Experimental)

*71Shi2: R. Shiromizu and Y. Mishima, "Reversion of Metastable Phases in Cu-Be Alloys," *J. Jpn. Inst. Met.*, *35*, 183-189 (1971) in Japanese. (Meta Phases, Experimental; #)

71Yam: S. Yamamoto, M. Matsui, and Y. Murakami, "Electron Microscopic Observation on Precipitation Sequence in Cu-Be Alloys," *Trans. Jpn. Inst. Met.*, *12*, 159-165 (1971). (Meta Phases, Crys Structure; Experimental)

73Phi: V.A. Phillips and L.E. Tanner, "High Resolution Electron Microscope Observations on GP Zones in Aged Cu-1.97 wt.% Be Crystal," *Acta Metall.*, *21*, 441-448 (1973). (Meta Phases; Experimental)

73Tad: T. Tadaki, T. Sahara, and K. Shimizu, "Electron Metallography of Decomposition Processes in Hyper-Eutectoid Cu-Be β Phase Alloy," *Trans. Jpn. Inst. Met.*, *14*(5), 401-407 (1973). (Equi Diagram; Meta Phases, Crys Structure; Experimental)

*73Tya1: Yu.D. Tyapkin and V.A. Golikov, "Crystallostructural Investigation of Eutectoid Decomposition of Cu-Be Alloys. Ordering with Formation of Mestable Solid Solution Cu_2Be," *Fiz. Meta. Metalloved.*, *35*,336-346 (1973) in Russian: TR: *Phys. Met. Metallogr.*, *35*(2), 101-110 (1973). (Meta Phases, Crys Structure; Experimental)

73Tya2: Yu.D. Tyapkin and V.A. Golikov, "Crystallographic Investigation of Eutectoid Disintegration of Cu-Be Alloys. Structural changes of β″ phase to Cu_2Be in Course of Ordering," *Fiz. Metal. Metalloved.*, *36*, 1058-1070 (1973) in Russian; TR: *Phys. Met. Metallogr.*, *36*(5), 144-154 (1973). (Meta Phases, Crys Structure; Experimental)

*74Auv: X. Auvray, R. Graf, and A. Guinier, "Study of Cu-Be Alloys Close to the Eutectoid Composition," *Scr. Metall.*, *8*, 995-1004 (1974) in French. (Meta Phases, Crys Structure; Experimental)

*74Bon1: W. Bonfield and B.C. Edwards, "Precipitation Hardening in Cu-1.81 wt.% Be-0.28 wt.% Co, Part 1: Continuous Precipitation," *J. Mater. Sci.*, *9*, 398-408 (1974). (Meta Phases, Crys Structure; Experimental)

*74Bon2: W. Bonfield and B.C. Edwards, "Precipitation Hardening in Cu-1.81 wt.% Be-0.28 wt.% Co, Part 2: Discontinuous Precipitation," *J. Mater. Sci.*, *9*, 409-414 (1974). (Equi Diagram; Experimental)

*74Gol: V.A. Golikov and Yu.D. Tyapkin, "Crystallographic Analysis of Eutectoid Decomposition of Cu-Be Alloys. Initial

Stages of Decomposition," *Fiz. Metal. Metalloved.*, *37*, 322-327 (1974) in Russian; TR: *Phys. Met. Metallogr.*, *37*(2), 89-93 (1974). (Meta Phases, Crys Structure; Experimental)

74Gri: R.B. Griffiths, "Thermodynamic Model for Tricritical Points in Ternary and Quaternary Fluid Mixtures," *J. Chem. Phys.*, *60*(1), 195-206 (1974). (Thermo; Theory)

74Tya1: Yu.D. Tyapkin, V.A. Golikov, A.V. Gavrilova, and V.D. Vasin, "New Type of Quasiperiodical (Modulated) Structure in Aging and Eutectoid Alloys," *Scr. Metall.*, *8*(10), 1171-1174 (1974). (Equi Diagram; Experimental)

74Tya2: Yu.D. Tyapkin and V.A. Golikov, "Development of Quasi Periodical Distribution of Nuclei in Sites of Tetragonal Body Centered Macrolattice during Eutectoid Decomposition of Cu-Be Alloys," *Fiz. Metal. Metalloved.*, *38*, 803-811 (1974) in Russian; TR: *Phys. Met. Metallogr.*, *38*(4), 117-123 (1974). (Equi Diagram; Experimental)

***75Rak:** A.G. Rakhshtadt and Kh.G. Tkhagapsoyev, "Relationships Governing Discontinuous Decomposition of α Solid Solution in Cu-Be Alloys," *Izv. Akad. Nauk SSSR, Met.*, *6*, 188-195 (1975) in Russian; TR: *Russ. Metall.*, *6*, 150-156 (1975). (Equi Diagram; Experimental)

76All: S.M. Allen and J.W. Cahn, "Mechanisms of Phase Transformations within Miscibility Gap of Fe-Rich Fe-Al Alloys," *Acta Metall.*, *24*, 425-437 (1976). (Equi Diagram; Thermo; Theory)

***77Auv:** X. Auvray, "Study of Cu-Be Alloys Near Eutectoid Composition," Sc.D. thesis, Univ. Rouen, France (1977). (Meta Phases; Equi Diagram, Experimental)

77Mye: S.M. Myers and J.E. Smugeresky, "Low Temperature Solubility of Cu in Be, in Be-Al, and in Be-Si using Ion Beams,"*Metall. Trans. A*, *8*, 609-616 (1977). (Equi Diagram; Experimental)

78Ino: H. Ino, "Pairwise Interaction Model for Decomposition and Ordering Processes in BCC Binary Alloys and its Application to Fe-Be System," *Acta Metall.*, *26*, 827-834 (1978). (Equi Diagram; Thermo; Theory)

78Tsu: H. Tsubakino and R. Nozato, "On Relationship between Discontinuous Precipitation and Continuous Precipitation in Cu-Be Alloys," *Bull. Univ. Osaka Prefecture Ser. A*, *27*(2), 149-165 (1978). (Equi Diagram; Experimental)

78Wil: D.B. Williams, "Analytic TEM of Discontinuous Reaction in Cu-Be-Co Alloys," *Ninth Int. Cong. Electron Microscopy (Toronto)*, *1*, 506-507 (1978). (Equi Diagram; Experimental)

79Ald: F. Aldinger and G. Petzow, in *Beryllium Science and Technology*, Vol. 1, D. Webster and G.L. London, Ed., Plenum Press, New York, 235-305 (1979). (Equi Diagram; Review; #)

79Bab: E.G. Baburaj, U.D. Kulkarni, E.S.K. Menon, and R. Krishnan, "CuBe Precipitation in Cu-Be Alloys," *Phase Transform.*, *1*, 171-198 (1979). (Meta Phases; Experimental)

79Rio: R.J. Rioja, Ph.D. thesis, Carnegie Mellon University, Met. Eng. and Mat. Sci., Pittsburgh, PA (1979). (Equi Diagram; Experimental)

80Bau: S.F. Baumann and D.B. Williams, "Suppression of Discontinuous Reaction in Cu-Be Alloys," *Electron Microscopy*, *1*, 194-195 (1980). (Equi Diagram; Experimental)

80Gie: W.C. Giessen, "Be-Cu System," *Bull. Alloy Phase Diagrams*, *1*(1), 50-52 (1980). (Meta Phases; Experimental)

***80Rio:** R.J. Rioja and D.E. Laughlin, "Sequence of Precipitation in Cu-2 wt.% Be Alloys," *Acta Metall.*, *28*, 1301-1313 (1980). (Meta Phases, Crys Structure; Experimental)

80Tsu: H. Tsubakino, R. Nozato, and H. Mitani, "Influence of Co on Volume Fraction of Discontinuous Precipitation Cells in Cu-2 wt.% Be-Co Alloys," *J. Jpn. Inst. Met.*, *44*(10), 1122-1126 (1980) in Japanese. (Equi Diagram; Experimental)

***81Lau:** D.E. Laughlin and L.E. Tanner, "The Be-Cu System: Metastable Solvi," *Bull. Alloy Phase Diagrams*, *2*(1), 28 (1981). (Meta Phases; Experimental; #)

81Sva: L.S. Svanidze, V.A. Golikov, and Yu.D. Tyapkin, "On Nature of Surface Relief Resulting from Eutectoid Decomposition of Alloys Cu-Be and Aging of Alloys Cu-Be, Ni-Be," *Fiz. Met. Metalloved.*, *51*, 883-887 (1981) in Russian; TR: *Phys. Met. Metallogr.*, *51*(4), 185-189 (1981). (Meta Phases, Crys Structure; Experimental)

82Ale: K.B. Alexander, D.A. Steigerwald, and D.E. Laughlin, "Effect of Continuous Precipitation Kinetics on Discontinuous Precipitation in Cu-Be and Al-Ag Alloys," Proc. Int. Conf., Carnegie Mellon University, Aug 1981, in *Solid-Solid Phase Transformations*, H.I. Aaronson, D.E. Laughlin, R.F. Sekerka, and C.M. Wayman, Ed., AIME, 945-949 (1982). (Equi Diagram; Experimental)

82All: S.M. Allen and J.W. Cahn, "Phase Diagram Features Associated with Multicritical Points in Alloy Systems," *Bull. Alloy Phase Diagrams*, *3*(3), 287-295 (1982). (Equi Diagram; Theory)

82Gar: J. Garcia, R.J. Rioja, and D.E. Laughlin, private communication (1982). (Equi Diagram; Experimental; #)

***82Jon:** S. Jonsson, K. Kaltenbach, and G. Petzow, "Phase Relations in Be-Rich Section of Be-Cu-Fe System," *Z. Metallkd.*, *73*(8), 534-539 (1982). (Equi Diagram; Experimental; #)

82Kal: K. Kaltenbach, private communication of tabulated data from [82Jon] and from some more recent measurements.

82Sof: W.A. Soffa and D.E. Laughlin, "Recent Experimental Studies of Continuous Transformations in Alloys: An Overview," Proc. Int. Conf., Carnegie Mellon University, Aug 1981, in *Solid-Solid Phase Transformations*, H.I. Aaronson, D.E. Laughlin, R.F. Sekerka, and C.M. Wayman, Ed., AIME, 159-183 (1982). (Thermo; Review)

82Tan: L.E. Tanner, A.R. Pelton, and R. Gronsky, Characterization of Pre-Transformation Morphologies: Periodic Strain Modulations," ICOMAT '82, Belgium (1982); preprint. (Equi Diagram; Experimental)

83Mik: M. Miki, S. Hori, and Y. Amano, "Effect of Additional Elements on Grain Boundary Reaction in Cu-2 wt.% Be Alloy," *Trans. Jpn. Inst. Met.*, *24*, 674-680 (1983). (Equi Diagram, Meta Phases; Experimental)

84Kau: L. Kaufman and L.E. Tanner, "Coupled Phase Diagrams and Thermochemical Descriptions of Fe-Be, Co-Be, Ni-Be, and Cu-Be Systems," *Calphad*, *8*(2), 121-133 (1984). (Thermo; Theory)

86Koo: Y.M. Koo, diss., Northwestern University (1986). (Meta Phases; Experimental)

*Indicates key paper.
*Indicates presence of a phase diagram.

Be-Cu evaluation contributed by **D.J. Chakrabarti,** Alcoa Research Laboratories, Alcoa Technical Center, Alcoa Center, PA 15069, USA, **D.E. Laughlin,** Department of Metallurgical Engineering and Materials Science, Carnegie Mellon University, Pittsburgh, PA 15213, USA, and **L.E. Tanner,** Lawrence Livermore Laboratory, Livermore, CA 94550, USA. Work was supported by the International Copper Research Association, Inc. (INCRA) and the Department of Energy through the Joint Program on Critical Compilation of Physical and Chemical Data coordinated through the Office of Standard Reference Data (OSRD), National Bureau of Standards. Literature searched through 1983. Professor Laughlin is the ASM/NBS Data Program Category Editor for binary copper alloys, and Mr. Tanner is the Co-Category Editor for binary beryllium alloys.